

# Polymer-composite fibers for transmitting high peak power pulses at 1.55 microns

Zachary Ruff,<sup>1</sup> Dana Shemuly,<sup>1</sup> Xiang Peng,<sup>2</sup> Ofer Shapira,<sup>1</sup> Zheng Wang,<sup>1</sup>  
and Yoel Fink<sup>1,\*</sup>

<sup>1</sup>Research Laboratory of Electronics and Department of Materials Science and Engineering, Massachusetts Institute of Technology, Cambridge, Massachusetts, 02139, USA

<sup>2</sup>Raydiance Inc. 2199 S. McDowell Blvd. Suite 140 Petaluma, California 94954, USA  
[\\*yoel@mit.edu](mailto:yoel@mit.edu)

**Abstract:** Hollow-core photonic bandgap fibers (PBG) offer the opportunity to suppress highly the optical absorption and nonlinearities of their constituent materials, which makes them viable candidates for transmitting high-peak power pulses. We report the fabrication and characterization of polymer-composite PBG fibers in a novel materials system, polycarbonate and arsenic sulfide glass. Propagation losses for the 60 $\mu$ m-core fibers are less than 2dB/m, a 52x improvement over previous 1D-PBG fibers at this wavelength. Through preferential coupling the fiber is capable of operating with over 97% the fiber's power output in the fundamental ( $HE_{11}$ ) mode. The fiber transmitted pulses with peak powers of 11.4 MW before failure.

© 2010 Optical Society of America

**OCIS Codes:** (060.2280) Fiber design and fabrication; (160.5293) Photonic bandgap materials; (060.2290) Fiber materials.

---

## References and links:

1. B. Richou, I. Schertz, I. Gobin, and J. Richou, "Delivery of 10-MW Nd:YAG laser pulses by large-core optical fibers: dependence of the laser-intensity profile on beam propagation," *Appl. Opt.* **36**(7), 1610–1614 (1997).
2. Y. Matsuura, K. Hanamoto, S. Sato, and M. Miyagi, "Hollow-fiber delivery of high-power pulsed Nd:YAG laser light," *Opt. Lett.* **23**(23), 1858–1860 (1998).
3. S. O. Konorov, V. P. Mitrokhin, A. B. Fedotov, D. A. Sidorov-Biryukov, V. I. Beloglazov, N. B. Skibina, A. V. Shcherbakov, E. Wintner, M. Scalora, and A. M. Zheltikov, "Laser ablation of dental tissues with picosecond pulses of 1.06-microm radiation transmitted through a hollow-core photonic-crystal fiber," *Appl. Opt.* **43**(11), 2251–2256 (2004).
4. N. K. T. Photonics, Data sheet. <http://www.nktp Photonics.com/>, Accessed November 2009.
5. S. G. Johnson, M. Ibanescu, M. Skorobogatiy, O. Weisberg, T. D. Engeness, M. Soljacic, S. A. Jacobs, J. D. Joannopoulos, and Y. Fink, "Low-loss asymptotically single-mode propagation in large-core OmniGuide fibers," *Opt. Express* **9**(13), 748–779 (2001).
6. P. Yeh, A. Yariv, and E. Marom, "Theory of Bragg fiber," *J. Opt. Soc. Am.* **68**(9), 1196–1201 (1978).
7. Y. Fink, J. N. Winn, S. Fan, C. Chen, J. Michel, J. D. Joannopoulos, and E. L. Thomas, "A dielectric omnidirectional reflector," *Science* **282**(5394), 1679–1682 (1998).
8. Y. Fink, D. J. Ripin, S. Fan, C. Chen, J. D. Joannopoulos, and E. L. Thomas, "Guiding optical light in air using an all-dielectric structure," *J. Lightwave Technol.* **17**(11), 2039–2041 (1999).
9. K. Kuriki, O. Shapira, S. Hart, G. Benoit, Y. Kuriki, J. Viens, M. Bayindir, J. Joannopoulos, and Y. Fink, "Hollow multilayer photonic bandgap fibers for NIR applications," *Opt. Express* **12**(8), 1510–1517 (2004).
10. B. Temelkuran, S. D. Hart, G. Benoit, J. D. Joannopoulos, and Y. Fink, "Wavelength-scalable hollow optical fibres with large photonic bandgaps for CO<sub>2</sub> laser transmission," *Nature* **420**(6916), 650–653 (2002).
11. T. Engeness, M. Ibanescu, S. Johnson, O. Weisberg, M. Skorobogatiy, S. Jacobs, and Y. Fink, "Dispersion tailoring and compensation by modal interactions in OmniGuide fibers," *Opt. Express* **11**(10), 1175–1196 (2003).
12. O. Shapira, K. Kuriki, N. D. Orf, A. F. Abouraddy, G. Benoit, J. F. Viens, A. Rodriguez, M. Ibanescu, J. D. Joannopoulos, Y. Fink, and M. M. Brewster, "Surface-emitting fiber lasers," *Opt. Express* **14**(9), 3929–3935 (2006).
13. E. Bychkov, M. Miloshova, D. L. Price, C. J. Benmore, and A. Lorriaux, "Short, intermediate and mesoscopic range order in sulfur-rich binary glasses," *J. Non-Cryst. Solids* **352**(1 Issue 1), 63–70 (2006).
14. Z. U. Borisova, *Glassy Semiconductors* (Plenum, New York, 1981).
15. O. Shapira, A. F. Abouraddy, J. D. Joannopoulos, and Y. Fink, "Complete modal decomposition for optical waveguides," *Phys. Rev. Lett.* **94**(14), 143902 (2005).

16. V. Nguyen, F. Sanghera, B. Cole, P. Pureza, F. H. Kung, and I. D. Aggarwal, "Fabrication of Arsenic Sulfide Optical Fiber with Low Hydrogen Impurities," *J. Am. Ceram. Soc.* **85**(8), 2056–2058 (2002).
  17. A. Mendez and T. F. Morse, *Specialty Optical Fibers Handbook* (Elsevier, 2007).
  18. D. G. Ouzounov, F. R. Ahmad, D. Müller, N. Venkataraman, M. T. Gallagher, M. G. Thomas, J. Silcox, and K. W. Koch, "A. L. Gaeta\* "Generation of Megawatt Optical Solitons in Hollow-Core Photonic Band-Gap Fibers," *Science* **1702**, 301 (2003).
  19. A. V. Smith, and B. T. Do, "Bulk and surface laser damage of silica by picosecond and nanosecond pulses at 1064 nm," *Appl. Opt.* **47**(26), 4812–4832 (2008).
  20. J. D. Shephard, F. Couny, P. S. Russell, J. D. C. Jones, J. C. Knight, and D. P. Hand, "Improved hollow-core photonic crystal fiber design for delivery of nanosecond pulses in laser micromachining applications," *Appl. Opt.* **44**(21), 4582–4588 (2005).
  21. M. Borghesi, A. J. Mackinnon, R. Gaillard, O. Willi, and A. A. Offenberger, "Guiding of a 10-TW picosecond laser pulse through hollow capillary tubes," *Phys. Rev. E Stat. Phys. Plasmas Fluids Relat. Interdiscip. Topics* **57**(5), R4899–R4902 (1998).
- 

## 1. Introduction

High-peak power laser pulses in the near infrared (NIR) have important medical, industrial and military applications. In conventional single-mode silica fibers, the damage threshold due to the core material's finite optical absorption, and the pulse distortion induced by the core material's self-phase modulation limit the transmitted peak power. To reduce the optical power density in the core, large mode-area silica fibers have been developed, but poor-mode quality, peak-power limitations and coupling instabilities limit their suitability for many applications [1]. An alternative approach is to guide the pulse using a mirror or a photonic crystal, eliminating the core material. Large-core hollow fibers such as polymer-metal waveguides have been shown to transmit high-peak power pulses, but poor mode quality too restricts their performance [2]. Air-silica 2D-photonic crystal fibers (PCF) can deliver pulses without compromising mode-quality, though they can have a somewhat limited damage threshold, since even commercially optimized designs confine only ~98% of the transmitted power to the air-core of the fiber [3,4,18,20]. In this paper, we will show that 1D-PCF or photonic bandgap (PBG) fibers can strongly confine light to a hollow core, suppressing materials absorption and nonlinearities by over 5 orders of magnitude, while still delivering mode qualities approaching that of a step-index single mode fiber [5].

Previous investigations have demonstrated some of the unique properties and potential uses of PBG fibers [6–12]. High-index contrast structures demonstrate omni-directional reflectivity [7] and can be incorporated into optical fibers by co-drawing a low-index polymer with a high-index chalcogenide glass [8]. By simply scaling the dimensions of the bi-layer structures, the co-drawing technique has been used to draw fibers that transmit light from the less than 1 $\mu\text{m}$  out past 10 $\mu\text{m}$ , suppressing the relatively high absorption losses of the constituent materials [9,10]. Cavities can also be introduced into the fibers in order to tailor dispersion for applications such as dispersion compensation and pulse compression [11].

Earlier investigations into polymer-composite fibers used high temperature thermoplastics, such as polyethersulfone (PES) and polyetherimide (PEI) that have relatively high extinction coefficients compared to more common optical polymers. In this work, we demonstrate that optical polymers with lower extinction coefficients can be used to further reduce the absorption losses of PBG fibers. We chose polycarbonate over other amorphous optical polymers, such as Cyclic-Olefin copolymers, due to its commercial availability at experimentally favorable film thicknesses. Polycarbonate's extinction coefficient at 1.55 $\mu\text{m}$  is over an order of magnitude less than either PES's or PEI's coefficient (Fig. 4a), pushing the absorption loss limit for PBG fibers below 0.05 dB/m for a 60 $\mu\text{m}$  core fiber. Polycarbonate also exhibits low absorption into the visible spectrum, creating the opportunity for low-loss fibers with bandgaps approaching the UV. For this work, we were able only to source films extruded from a general use polycarbonate resin (Lexan 104), which contained significant inclusions (dust, poor molecular weight distribution). We expect an optical grade film to further improve transmission losses.

## 2. Material properties and device fabrication

Polycarbonate has a significantly lower glass transition temperature ( $T_g = 150\text{ }^\circ\text{C}$ ) than either PES ( $T_g \sim 220\text{ }^\circ\text{C}$ ) or PEI ( $T_g \sim 230\text{ }^\circ\text{C}$ ) making it incompatible to co-draw with commercial chalcogenide glasses, such as arsenic triselenide and arsenic trisulfide ( $\text{As}_2\text{S}_3$ ). By increasing the sulfur content in  $\text{As}_2\text{S}_3$  to  $\text{As}_{25}\text{S}_{75}$ , we reduced the  $T_g$  of the glass sufficiently to co-draw with polycarbonate, slightly decreasing the glass's index of refraction ( $n_{\text{As}_2\text{S}_3} = 2.4$ ,  $n_{\text{As}_{25}\text{S}_{75}} = 2.27$  at  $1.55\mu\text{m}$ ). However, polycarbonate ( $n = 1.53$ ) has a lower refractive index than either PES ( $n = 1.61$ ) or PEI ( $n = 1.66$ ) at  $1.55\mu\text{m}$ , which maintains a similar index contrast. For this work, we measured the index of refraction of polycarbonate and  $\text{As}_{25}\text{S}_{75}$  using a spectroscopic ellipsometer (Sopra).

$\text{As}_{25}\text{S}_{75}$  was synthesized in a rocking furnace using the melt-quench technique from as received elemental sulfur (5N5 Alfa Aesar) and elemental arsenic (7N5 UMC Corp.), heated under vacuum to remove surface oxides. Differential scanning calorimetry ( $10\text{ C min}^{-1}$ , TA instruments DSC Q1000) shows a single glass transition temperature ( $T_g \sim 120\text{ C}$ ) and no crystallization peaks, despite some evidence in the literature that  $\text{As}_{25}\text{S}_{75}$  can phase separate [13]. Thermal gravitational analysis ( $10\text{ C min}^{-1}$ , TA Instruments Q50) shows that the glass thermally decomposes continuously from the melt with a single peak, supporting that the glass is a single phase. The extinction coefficient of the synthesized glass is significantly higher than what we would expect from further purification, but is nonetheless negligible compared to the polymer's coefficient (Fig. 4a) [16].

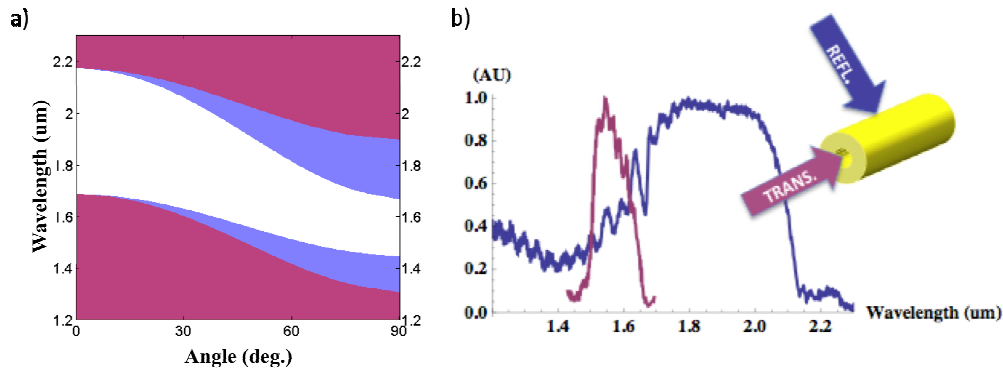


Fig. 1. (a) Simulated band diagram for an ideal PBG structure of  $\text{As}_{25}\text{S}_{75}$  and polycarbonate with a fundamental bandgap centered at  $1.55\mu\text{m}$ . Regions with propagating modes are shaded (blue for TM, red for TE and purple for both) (b) Measured transmission ( $\theta = 90$ ) and reflection ( $\theta = 0$ ) bandgaps for the PBG fiber described in this paper.

Glass/Polymer bilayers were obtained using a custom roll-to-roll thermal evaporator. During the deposition, a polymer web passes over two sets of evaporator boats, allowing glass to be deposited independently on either side of the film. In order to minimize the penetration depth of the  $\text{HE}_{11}$  mode into the bilayer structure, the glass was deposited at  $1/3$  of a full glass layer thickness on the inner surface and  $2/3$  at the outer layer [16]. Electron microprobe analysis (JEOL JXA-733) showed that the arsenic content increases during the evaporation from  $\text{As}_{25}\text{S}_{75}$  ( $+ -0.5\text{ mol } \%$ ) to  $\text{As}_{28}\text{S}_{72}$  ( $+ -1.0\text{ mol } \%$ ). This is not surprising, since the glass decomposes from the melt into an arsenic rich vapor ( $\text{As}_{25}\text{S}_{75} \rightarrow \text{As}_4\text{S}_4 + \text{S}_2$  [14]) and sulfur gas, which can be pulled from the chamber.

The bilayer film and additional polycarbonate cladding films were rolled onto a mandrel and heated under vacuum to  $185\text{ C}$ , fusing the films into a preform. The preform was then drawn into a fiber between  $245$  and  $265\text{ C}$ , while the fiber's outer diameter, core-size and stress were closely monitored. Pressure was applied to the core, in order to keep the core from collapsing due to surface energy. Any change between the ratio of the outer and inner

diameter of the preform to the fiber (normalize-shrink down ratio or NS) would chirp the thickness of the bilayers, decreasing the fiber's spectral bandwidth. The standard deviation of the fiber's outer diameter was monitored using a laser micrometer and was controlled to less than  $\pm 1\%$  ( $\pm 7 \mu\text{m}$ ). A FTIR microscopy (Bruker, Tensor 37) was used to measure radial reflections off the outer surface of the core. Measurements showed a clear bandgap with interference side-bands, indicative of a well ordered-periodic structure (Fig. 1b). The fiber's axial transmission spectrum was also monitored to ensure the correct position of the fiber's transmission bandgap using an infrared spectrometer (Photon control, SPM-002 NIR1700).

### 3. Measurements and results

Scanning electron microscopy (SEM, JEOL 6060) images show that the preform's geometry is maintained through the fiber drawing process (Fig. 2). The 760-micron outer diameter fiber has a NS of 1 and a 60-micron core ( $40\lambda$  at  $1.5\mu\text{m}$ ). The images show smooth interfaces between the glass and polymer layers. Fourier analysis on the SEM image of the 22 glass-polymer bilayers reveals a sharp peak at 521nm, agreeing strongly with our simulations. There is a tight distribution in the bilayer thickness with a full-width at half-maximum (FWHM) of 27nm, which is below the resolution of the SEM image.

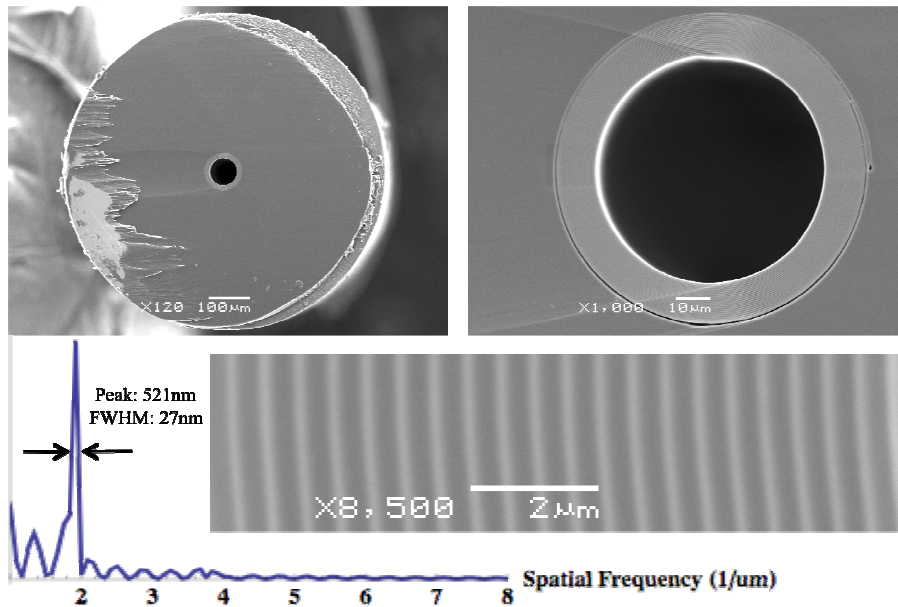


Fig. 2. Cross-sectional SEM images of a PBG fiber with a 60 $\mu\text{m}$ -core, a 760 $\mu\text{m}$  outer diameter and Fourier analysis of the glass-polymer bilayers.

Propagation loss measurements were performed using the cutback method. The output of a single mode fiber coupled to a frequency-swept laser source from 1520nm-1620nm (Ando) provided a linear polarized Gaussian beam for the measurement. A spherical lens coupled the beam preferentially into the  $\text{HE}_{11}$  mode; the fiber's lowest order linearly polarized mode. A 2-meter section of fiber was held straight and cutback five times to 1-meter. Over the 100nm bandwidth of the laser, the propagation losses are from 2 to 3 dB/m, with a minimum loss of less than 2dB/m at 1560nm (Fig. 4a). The propagation losses are a significant improvement over previously published work of 5.5 dB/m for a 160 $\mu\text{m}$ -core fiber. Absorption and scattering losses scale as  $1/R^3$ , corresponding to a 52x improvement compared to the fiber in this work [17].

The modal content of the fiber's output was analyzed using a mode decomposition algorithm described in our previous work (Fig. 3) [15]. Reducing the fiber's core-size limits

modal coupling, since the spacing between modes scale as  $1/R^2$  [5]. Unlike previously demonstrated NIR fibers with larger cores, the modal content at the output of these fibers is over 97%  $HE_{11}$ . Since the  $HE_{11}$  mode overlaps strongly with a Gaussian beam, the fiber's output can be highly focused for applications where power density is critical. Another consequence of the increased mode spacing is that no additional bending losses were observed down to radii sufficient to damage the fiber mechanically ( $\sim 2\text{cm}$ ), when careful attention is paid to maintain the input coupling.

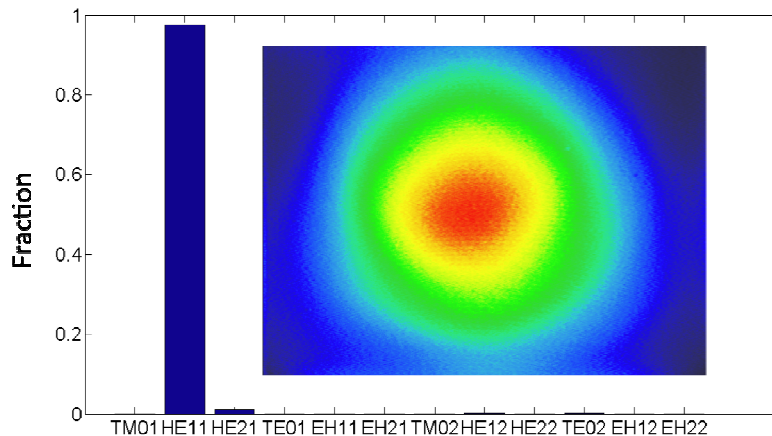


Fig. 3. Far-Field intensity distribution at the output of the PBG fiber after 1-meter, excited at  $1.55\mu\text{m}$  and the proportional modal content of the first 12 modes as determined by the modal-decomposition algorithm.

Despite these improvements, the fiber still exhibits propagation losses for the  $HE_{11}$  mode two orders of magnitude greater than simulations that account for materials' absorption and the finite number of layers in the photonic crystal. An integrating sphere and detector were used to measure the power radiating from the fiber as the sphere was moved along the fiber. The radiation losses matched the propagation losses measured using the cutback technique. Therefore, scattering mechanisms such as interface roughness (air/core, bilayer) and inclusions (dust, phase separation) are likely limiting fiber performance and will be subject to further investigation. Each of these scattering mechanisms can potentially couple light from the  $HE_{11}$  to either higher-order or cladding modes. Nonetheless, the high modal purity is maintained at the fiber's output due to a modal filtering mechanism, where higher-order modes will have a higher differential loss than the fundamental mode [5].

Power handling measurements were performed using a laser source delivering 1-ps,  $50\mu\text{J}$  pulses at  $100\text{kHz}$  centered at  $1.552\mu\text{m}$  (USP, Raydiance Inc.). The output of the laser was coupled to the fiber using a spherical lens. No additional beam shaping or end-facet protection, such as a ferrule or pinhole, was used. The input coupling efficiency was about 90% at low powers. The output of the PBG fiber was measured using an optical spectrum analyzer, an autocorrelator and power meter. A half-wave plate and polarizing beam-splitter were used to slowly increase the power coupled to the fiber until failure. Failure occurred at the end-facet at  $12.7\mu\text{J}$  corresponding to a peak power of  $11.4\text{MW}$  and an average power of  $1.14\text{W}$ . The peak power was calculated by dividing the product of the coupling efficiency and the average power by the product of the pulse's temporal width (FWHM) and the repetition rate of the source. The  $HE_{11}$  mode of a  $60\mu\text{m}$  core fiber has a mode field diameter of  $35\mu\text{m}$ , corresponding to a power density of  $1.2\text{TW}/\text{cm}^2$  in the fiber core. As the input power increased, there was no observable change in the pulse width or spectrum at the output of the fiber, suggesting non-linearities are not significant (Fig. 4b-c). The fiber's dispersion was measured to be  $9.6\text{ps-nm}/\text{km}$  (OVA-Luna), which may account for the slight temporal

broadening of the fiber's output with respect to the USP laser and appears to be independent of the input power.

To our knowledge, the highest reported peak-power for air-silica PCF fiber around 1.5 $\mu\text{m}$  is 2.4 MW at atmosphere, using 110-fs pulses and a 12.7 $\mu\text{m}$  core fiber [18]. We have not been able to find any studies that have determined the bulk damage threshold for silica at 1.55 $\mu\text{m}$  for comparison. However, the bulk damage threshold for silica at 1.064 $\mu\text{m}$  has recently been established to be in the 1.4 TW/cm<sup>2</sup> range for 14-ps pulses [19]. The damage threshold at the air-silica interface in solid-core silica fibers is considerably lower unless careful steps have been taken to completely eliminate surface roughness [19]. Simple 100 $\mu\text{m}$  glass capillaries can transmit pulse with peak-powers over 10TW, although their functionality is limited to transmission lengths of about 1cm due to their relatively high propagation losses [21].

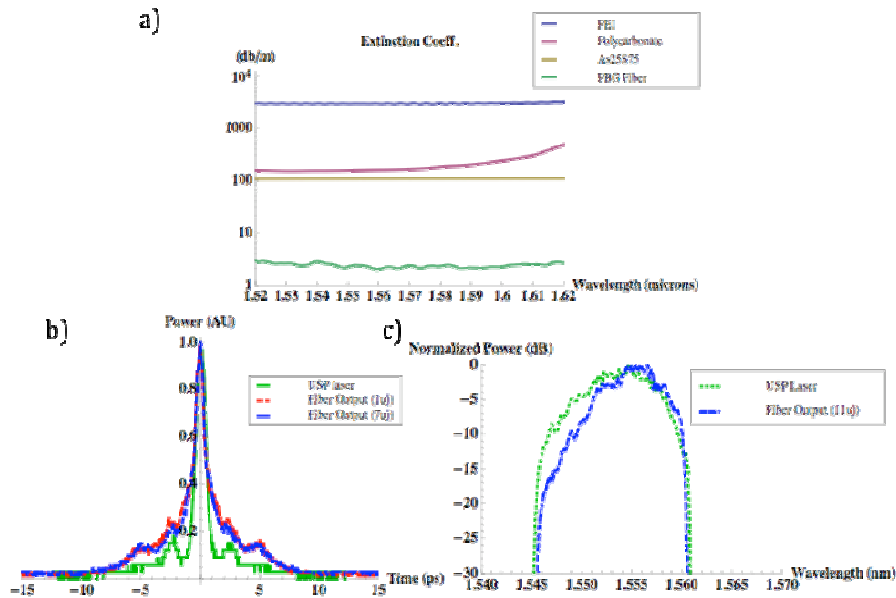


Fig. 4. (A) Extinction coefficients for materials and resultant fiber; all measurements were performed using the cutback method, (B) Autocorrelation traces of the USP laser and the fiber output, (C) OSA spectrum for the USP laser and the fiber output.

#### 4. Conclusions

We have fabricated PBG fibers in a new materials system, which has enabled the realization of fibers with 60 $\mu\text{m}$ -cores and propagation losses below 2dB/m. Through preferential coupling, these fibers can be used to transmit pulses with modal profiles approaching a single mode and peak-pulses up to 11.4 MW. Further investigations are required to study and to minimize scattering losses, which currently set the radiation-limited propagation losses for PBG fibers. Improving the input coupling should also increase the coupling efficiency and power-handling limit of the fibers. We believe that this work supports the viability of using polymer-composite PBG fibers to deliver high peak power pulses in the NIR.

#### Acknowledgments

This work was supported in part by the MRSEC Program of the National Science Foundation under award number DMR-0819762, the U.S Army Research Office through the Institute for Soldier Nanotechnologies under contract number W911NF-07-D-0004 and the Naval Air Warfare Center under contract N6833509C0013. Any opinions, findings and conclusions or

recommendations expressed in the material are those of the authors and do not necessarily reflect the views of the Naval Air Warfare Center.